scientific reports

Check for updates

OPEN

# Serum proteomic approach to identifying differentially expressed proteins in effusive feline infectious peritonitis

Wassamon Moyadee[1,2], Sittiruk Roytrakul[3], Janthima Jaresitthikunchai[3], Narumon Phaonakrop[3], Kiattawee Choowongkomon[4], Sekkarin Ploypetch[5], Natthasit Tansakul[6], Amonpun Rattanasrisomporn[7] & Jatuporn Rattanasrisomporn[1,2]✉

**Feline infectious peritonitis (FIP) is a lethal, viral-induced immune-mediated disease that remains a challenge for diagnosis and treatment in cats. Proteomic profiling, which analyzes the protein content of biological samples, offers the potential to identify novel biomarkers that could improve the diagnosis and management of FIP. This study aims to assess the serum proteome and identify proteins that differentiate healthy cats from cats diagnosed with effusive FIP using liquid chromatography coupled with tandem mass spectrometry (LC–MS/MS). A total of 30 cats diagnosed with effusive FIP and 27 clinically normal cats were enrolled. Twenty-three proteins were significantly ($p < 0.01$, ≥ fivefold change in abundance) differentially expressed between cats with effusive FIP and controls. Among these, the P2X purinoceptor, DNA topoisomerase, Notch receptor 2, and cadherin-17 were identified as key proteins of interest in cats with effusive FIP. Our findings suggest that these differentially expressed proteins could serve as potential diagnostic biomarkers and therapeutic targets for FIP. However, further studies are needed to validate these findings and explore their potential applications.**

**Keywords** Biomarkers, Cats, Coronavirus, Feline infectious peritonitis, Proteomics, Serum

Feline infectious peritonitis (FIP) is one of the most enigmatic and challenging diseases affecting domestic cats worldwide. First described in the early 1960s, FIP is caused by a feline coronavirus (FCoV) that mutates within the host. It is characterized by fibrinous and granulomatous serositis, immune-mediated vasculitis, protein-rich serous effusion in body cavities, and/or granulomatous lesions[1,2]. There are two forms of FIP, effusive (wet) and non-effusive (dry), which depend on the host's immune response[3]. In the past, there was no cure for FIP and no effective vaccine; the mortality rate was up to 100%. Recently, antiviral compounds, such as GS-441524, remdesivir, and molnupiravir, have been considered potential curative treatments for FIP[4,5]. However, descriptions of potential treatments are often based on cases without a diagnosis confirmed by immunohistochemistry (IHC).

Current diagnostic approaches for FIP involve a combination of clinical signs, laboratory tests, and imaging studies, allowing for the rapid and accurate diagnosis and initiation of treatment[6–8]. However, these approaches may lack the precision needed for a definitive and early diagnosis, particularly in the non-effusive form, which is the most challenging and difficult to diagnose. Various technologies have been explored for FIP diagnosis, including real-time quantitative reverse transcriptase-polymerase chain reaction (RT-PCR), loop-mediated isothermal amplification (LAMP), and enzyme-linked immunosorbent assay (ELISA)[9,10]. In the past, effusion and serological investigations and the measurement of acute phase proteins (APPs) in FIP were evaluated. Nevertheless, none of these can be recommended as a single definitive diagnostic test for FIP[9,11–13].

[1]Graduate Program in Animal Health and Biomedical Sciences, Faculty of Veterinary Medicine, Kasetsart University, Bangkok, Thailand. [2]Department of Companion Animal Clinical Sciences, Faculty of Veterinary Medicine, Kasetsart University, Bangkok, Thailand. [3]National Center for Genetic Engineering and Biotechnology, National Science and Technology Development Agency, Pathum Thani, Thailand. [4]Department of Biochemistry, Faculty of Science, Kasetsart University, Bangkok, Thailand. [5]Department of Clinical Sciences and Public Health, Faculty of Veterinary Science, Mahidol University, Nakhon Pathom, Thailand. [6]Department of Pharmacology, Faculty of Veterinary Medicine, Kasetsart University, Bangkok, Thailand. [7]Interdisciplinary of Genetic Engineering and Bioinformatics, Graduate School, Kasetsart University, Bangkok, Thailand. ✉email: fvejpn@ku.ac.th

Proteomic research provides insights into host–pathogen interactions, identifying biomarkers and elucidating molecular mechanisms[14]. Biomarkers in viral infections, such as human immunodeficiency virus (HIV), severe acute respiratory syndrome coronavirus 2 (SARS-CoV-2), and dengue virus (DENV), have been assessed. Chronic viral infections trigger immune system activation and inflammation, potentially leading to complications in noninfectious diseases[15–17]. Routine blood tests are simple, cost-effective, and widely used in veterinary medicine, making serum an ideal sample for analysis. In cats, serum and plasma proteomics have been explored in areas such as pancreatic diseases, chronic enteropathies, chronic kidney disease, and hypertrophic cardiomyopathy using liquid chromatography tandem mass spectrometry (LC–MS/MS), with or without matrix-assisted laser desorption/ionization time-of-flight mass spectrometry (MALDI-TOF MS)[18–21]. As of our last knowledge update, this study is the first to specifically investigate changes in serum protein patterns in cats with naturally occurring effusive FIP. It provides valuable preliminary data on protein markers that distinguish clinically normal cats from those with effusive FIP and may contribute to the diagnosis of non-effusive FIP.

## Materials and methods

### Animals and sampling

All samples were collected from the Kasetsart University Veterinary Teaching Hospital (KUVTH). Two main groups of cats were diagnosed and categorized as the control (non-FIP) group and the FIP group, with random ages, sexes, and breeds. Thirty cats per group were chosen for proteomic analysis. This study was conducted in accordance with ARRIVE guidelines. The study received prior ethical approval from the Kasetsart University Institutional Animal Care and Use Committee (ACKU66-VET-019). The selection criteria for the FIP cats were based on multiple assessments that contributed to a high suspicion of FIP, following previously published literature[2,4–9]. These assessments included consistent medical history, signalment, clinical appearance, hematology/serum biochemistry, detection of any effusion via radiography and ultrasonography, Rivalta's test, fluid analysis and cytological examination of the effusion, detection of feline coronavirus antibody using the ImmunoComb test kit (Biogal Galed Laboratories, Israel), and detection of the FCoV antigen by RT-PCR. Although RT-PCR was performed in most cases, some samples yielded negative results, which is consistent with previous reports indicating the potential for false-negative findings due to low or fluctuating viral loads. Therefore, final inclusion as an FIP case was determined based on the overall consistency of clinical, laboratory, and imaging findings, and not solely on RT-PCR positivity. Due to limited facilities and the cat owners' refusal to undergo invasive diagnostic procedures or necropsy examinations, most cases were not confirmed by IHC. Cats that did not match the above criteria, based on their signalment, clinical signs, physical examination, blood profiles, imaging findings, or any other tests inconsistent with FIP, were categorized as unlikely to have FIP and were excluded from the study (the supplementary data for the cases are available). Cats in the control group, which were blood donor cats at KUVTH, had no clinical illness and exhibited normal limits of hematology and biochemistry parameters from routine testing, including blood urea nitrogen, creatinine, alanine aminotransferase, total protein, and albumin. Cats in both groups were also screened serologically for feline immunodeficiency virus (FIV) and feline leukemia virus (FeLV) using the Witness FeLV/FIV test kit; positive cats were excluded. Information on the ages, sexes, and breeds is presented in Table 1.

Blood samples were collected from all cats via jugular or saphenous venipuncture during their first visit to KUVTH, followed by centrifugation for serum separation. Nonhemolyzed samples with sufficient volume were selected, and the serum was stored at − 20 °C until analysis.

### Peptide analysis and sample grouping using MALDI-TOF

To reduce the multivariate nature of samples in the clinical study, sample grouping was performed using MALDI-TOF with a 337 nm nitrogen laser for desorption and ionization. The matrix used was alpha-cyano-4-hydroxycinnamic acid (CHCA). The samples were separated into proteins in the serum with a molecular weight < 30 kDa using Nanasep. Total protein concentration was measured using the Lowry method, with bovine serum albumin as the standard[22]. The proteins were detected in the range of molecular ion peaks from m/z 1 to 10 kDa, with 500 shots per spot in linear mode. The same representative serum peptide profile patterns from each sample were pooled for LC–MS/MS analysis. The MALDI-TOF spectra were imported into ClinProTools software for post-processing and the generation of peptide profiles. A dendrogram was created for group classification, and principal component analysis (PCA) was conducted to demonstrate clear group separation. Based on the clustering results, the samples were automatically classified into 11 FIP subgroups and 6 non-FIP subgroups. Three cats in the non-FIP group were excluded due to inconsistent clustering results, and 27 non-FIP cats were included in the final dataset.

| Group | Clinical appearance | No. of samples | Age (years) Mean ± SD | Sex (no. of samples) | Breed (no. of samples) |
|---|---|---|---|---|---|
| Non-FIP (Control) | Normal | 27 | 2.7 ± 1.48 | M (22), F (5) | Domestic shorthair (26)<br>American wirehair (1) |
| FIP | Peritoneal effusion (14)<br>Pleural effusion (15)<br>Both (1) | 30 | 2 ± 2.26 | M (20), F (10) | Domestic shorthair (25)<br>Persian (2)<br>Scottish fold (2)<br>British shorthair (1) |

**Table 1**. Case history. *F* female, *M* male.

## Peptide identification by LC–MS/MS

Briefly, 15 µg of pooled samples in each group (FIP and non-FIP) were mixed with loading buffer (0.5 M dithiothreitol [DTT], 10% w/v SDS, 0.4 M Tris–HCl pH 6.8, 50% v/v glycerol, 0.1 mg/mL bromophenol blue) and boiled at 90 °C for 5 min prior to separating on 12.5% SDS-PAGE (Atto, Tokyo, Japan). The gels were fixed using a solution comprising 50% methanol, acetic acid, and 37% formaldehyde before being scanned using a GS-710 scanner (Bio-Rad Laboratories, Benicia, CA, USA) and stored in 0.1% acetic acid. Subsequently, in-gel tryptic digestion was performed, where protein bands in each lane were partitioned into 22 segments and chopped into 1 $mm^3$ pieces. The gel pieces were dehydrated using 100% acetonitrile (ACN) and dried. Cysteines were reduced and alkylated by 10 mM DTT in 10 mM ammonium bicarbonate and 100 mM iodoacetamide in 10 mM ammonium bicarbonate, respectively, prior to dehydrating twice in 100% ACN. After trypsin digestion in 50 mM $NH_4HCO_3$ (pH 7.8) overnight at 37 °C, peptides were extracted from the gels using 50% ACN in 0.1% formic acid (FA). Pooled samples were subjected to reversed-phase high-performance liquid chromatography (HPLC). The gradient-eluted peptides were analyzed using an Ultimate 3000 LC System coupled to an HCTUltra PTM Discovery System (Bruker Daltonics, Bremen, Germany). Peptides were separated on a PepSwift monolithic column (100 µm internal diameter × 50 mm; Thermo Fisher Scientific). Peptide separation was achieved with a linear gradient at a flow rate of 1000 nL/min from 4% ACN, 0.1% FA to 70% ACN, 0.1% FA for 7.5 min with a regeneration step at 90% ACN, 0.1% FA and an equilibration step at 4% ACN, 0.1% FA. The entire process took 20 min. Peptide fragment mass spectra were acquired in a data-dependent Auto MS mode with a scan range of 400–1500 m/z. However, when there were more than 5 precursor fragments, peptides were selected from the MS scan at 200–2800 m/z.

The CompassXport software (Bruker Daltonics) was used to convert data from LC–MS/MS into mzXML format. Protein quantitation was performed using the DeCyder MS Differential Analysis software (DeCyderMS, GE Healthcare)[23,24]. The peptide sequences were searched against the NCBI Mammal database for protein identification using the MASCOT software, version 2.2 (Matrix Science, London, UK)[25]. The database query included taxonomy (*Felis catus*), enzyme (trypsin), variable modifications (oxidation of methionine residues), mass values (monoisotopic), protein mass (unrestricted), peptide mass tolerance (1.2 Da), fragment mass tolerance (± 0.6 Da), peptide charge state (1+, 2+, and 3+), and maximum number of missed cleavages. Proteins were identified from one or more peptides with an individual MASCOT score corresponding to $p < 0.05$. The proteins were annotated and analyzed for biological processes and molecular functions using UniProtKB/Swiss-Prot entries (http://www.uniprot.org/). Panther (http://www.pantherdb.org) was additionally used to classify proteins into biological processes, molecular functions, and signaling pathways. A hierarchical clustering heat map, partial least squares discriminant analysis (PLS-DA), and a volcano plot were generated using MetaboAnalyst 6.0 (http://www.metaboanalyst.ca/). The volcano plot was employed to identify significant proteins with a $p$ value < 0.01 and a fold change (FC) greater than 5. The interaction network of candidate proteins and drugs was explored using the STITCH program version 5.0 (http://stitch.embl.de/)[26]. The framework for proteomic analysis is shown in Fig. 1.

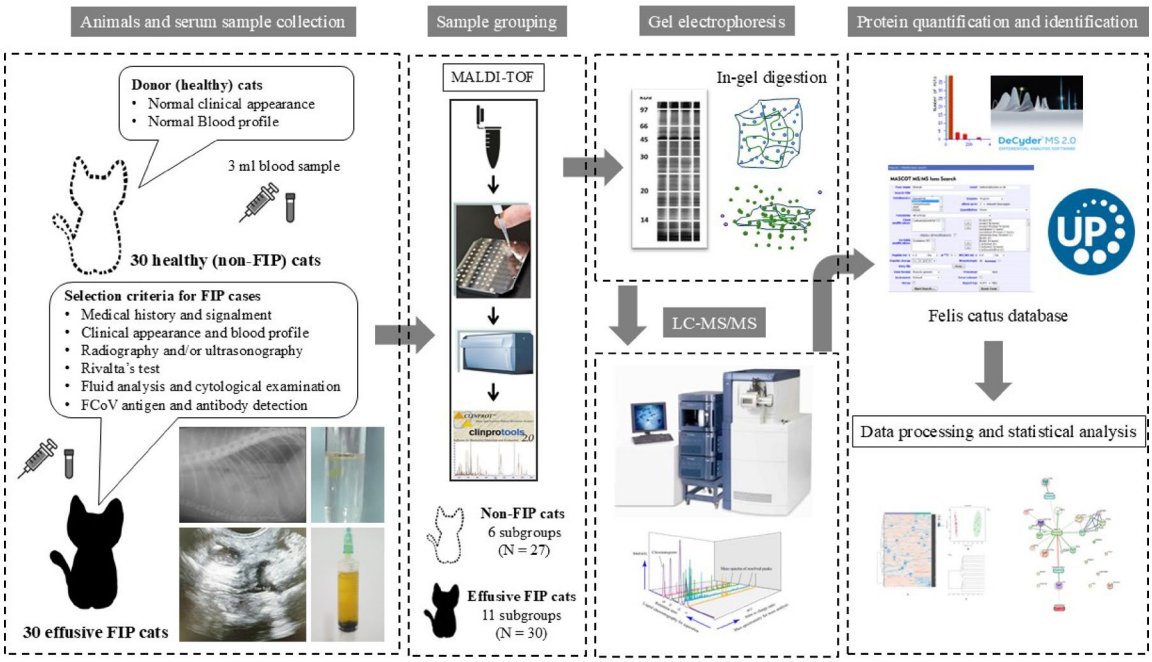


**Fig. 1**. Proteomic approach for serum analysis in effusive FIP. The proteomic workflow used to analyze serum samples from cats with effusive FIP and healthy cats for protein identification and quantification involves sample collection and preparation, protein extraction, LC–MS/MS, and bioinformatic analysis to identify and quantify differentially expressed proteins between the two groups.

# Results

## Sample description data

Of the 30 cats diagnosed with FIP, 83.3% were domestic shorthair (25/30), followed by 6.7% Persian (2/30), 6.7% Scottish fold (2/30), and 3.3% British shorthair (1/30). The mean age was 2 ± 2.26 years. Among these, 70% were male (21/30) and 30% were female (9/30). Regarding the 27 non-FIP cats, 81.5% were male, and 18.5% were female. The mean age was 2.7 ± 1.48 years, as described in Table 1.

## Peptide barcodes of FIP and non-FIP cats

After sample preparation, peptide masses < 30 kDa were collected and analyzed using the FlexAnalysis 3.4 and ClinProTool version 3.0 software (Bruker Daltonik, GmbH). Representative peptide mass fingerprint profiles obtained from MALDI-TOF analysis are shown in Fig. 2. The figure illustrates visible spectral differences between selected cats in the FIP and non-FIP groups. These examples were chosen to demonstrate distinct peptide pattern variations between groups, while comprehensive clustering and PCA analyses using all samples are presented in Fig. 3.

As described in the Methods, 27 non-FIP cats were ultimately included in the analysis and classified into six subgroups, while three were excluded due to inconsistent clustering. The FIP group comprised 30 cats, which were categorized into 11 subgroups. The PCA dimensional image (Fig. 3) illustrates a clear separation between the 11 FIP and 6 non-FIP subgroups.

## LC–MS/MS identification and quantitation of proteins in FIP and non-FIP cats

A total of 3384 proteins were identified from pooled LC–MS/MS analysis. Of these, 3379 proteins were detected in the FIP group and 3333 in the non-FIP group. Among these, 3328 proteins were shared between both groups, while 51 and 5 proteins were observed only in the FIP and non-FIP groups, respectively. The enrichment and differential expression analyses were based on the 3328 proteins commonly detected in both groups.

As shown in Fig. 4, in terms of biological processes, most identified proteins from FIP and non-FIP cats mainly belong to the cellular process (45.7% and 25.2%, respectively), biological regulation (32.2% and 17.7%, respectively), the metabolic process (20.7% and 11.4%, respectively), response to stimulus (14.3% and 4.9%, respectively), localization (22.5% and 6.9%, respectively), the developmental process (7.0% and 3.9%, respectively), the multicellular organismal process (6.67% and 3.7%, respectively), the homeostatic process (1.8% and 1.0%, respectively), the immune system process (1.3% and 0.7%, respectively), and the reproductive process (1.3% and 0.7%, respectively). In terms of molecular function, the proteins belongs to binding (30.5% and 25.1%, respectively), catalytic activity (19.7% and 16.2%, respectively), transcription regulator activity (6.6% and 5.4%, respectively), transporter activity (5.1% and 4.2%, respectively), molecular transducer activity (4.7% and 3.9%, respectively), molecular function regulator activity (4.4% and 3.6%, respectively), ATP-dependent activity (3.6% and 2.9%), structural molecule activity (2.0% and 1.6%, respectively), cytoskeletal motor activity (1.2% and 1.0%, respectively), and molecular adaptor activity (0.7% and 0.6%, respectively). Overall of the identified proteins, the proteins related to 10 main pathways, including the integrin signaling pathway (1.5% and 4.2%, respectively), the Wnt signaling pathway (1.4% and 4.0%, respectively), the gonadotropin-releasing hormone receptor pathway (1.2% and 3.4%, respectively), Huntington disease (1.2% and 3.4%, respectively), the inflammation mediated by chemokine and cytokine signaling pathway (1.1% and 3.3%, respectively), angiogenesis (0.9% and 2.7%, respectively), the nicotinic acetylcholine receptor signaling pathway (0.9% and 2.5%, respectively), the Alzheimer disease–presenilin pathway (0.8% and 2.2%, respectively), the platelet-derived growth factor (PDGF) signaling pathway (0.8% and 2.2%, respectively), and the epidermal growth factor (EGF) receptor signaling pathway (0.8% and 2.2%, respectively). Group-specific differences in biological processes, molecular functions, and signaling pathways between FIP and non-FIP cats are illustrated in Supplementary Figs. S1–S3.

The hierarchical clustering analysis was performed to study the first 30 proteins' differential expression profiles as heatmaps, shown in Fig. 5a. Each row in the heatmap represents a candidate protein, and each column

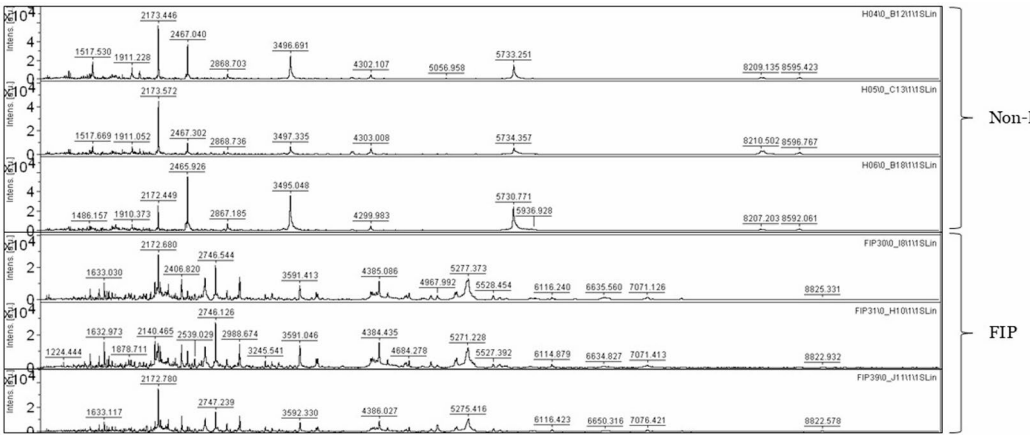


**Fig. 2**. Representative MALDI-TOF peptide fingerprint spectra from individual serum samples. Distinct mass pattern differences were observed between FIP and non-FIP cats.

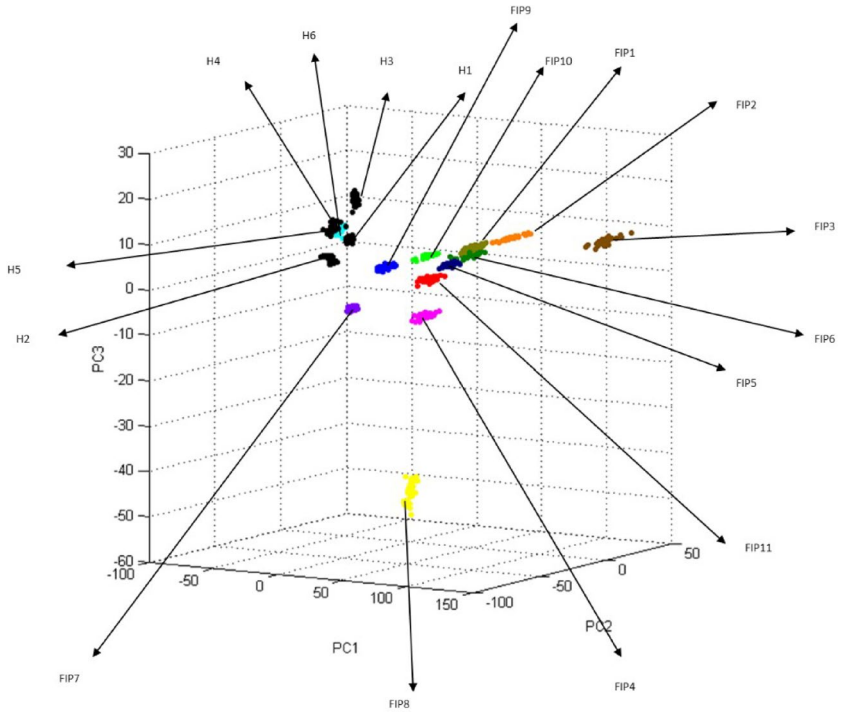


**Fig. 3**. The dimensional image from PCA showed the serum peptide profile distribution of all groups from MALDI-TOF spectra. The arrowheads labeled H1–H6 represent the cats in the non-FIP group, while the arrowheads labeled FIP1–FIP11 represent the cats in the FIP group.

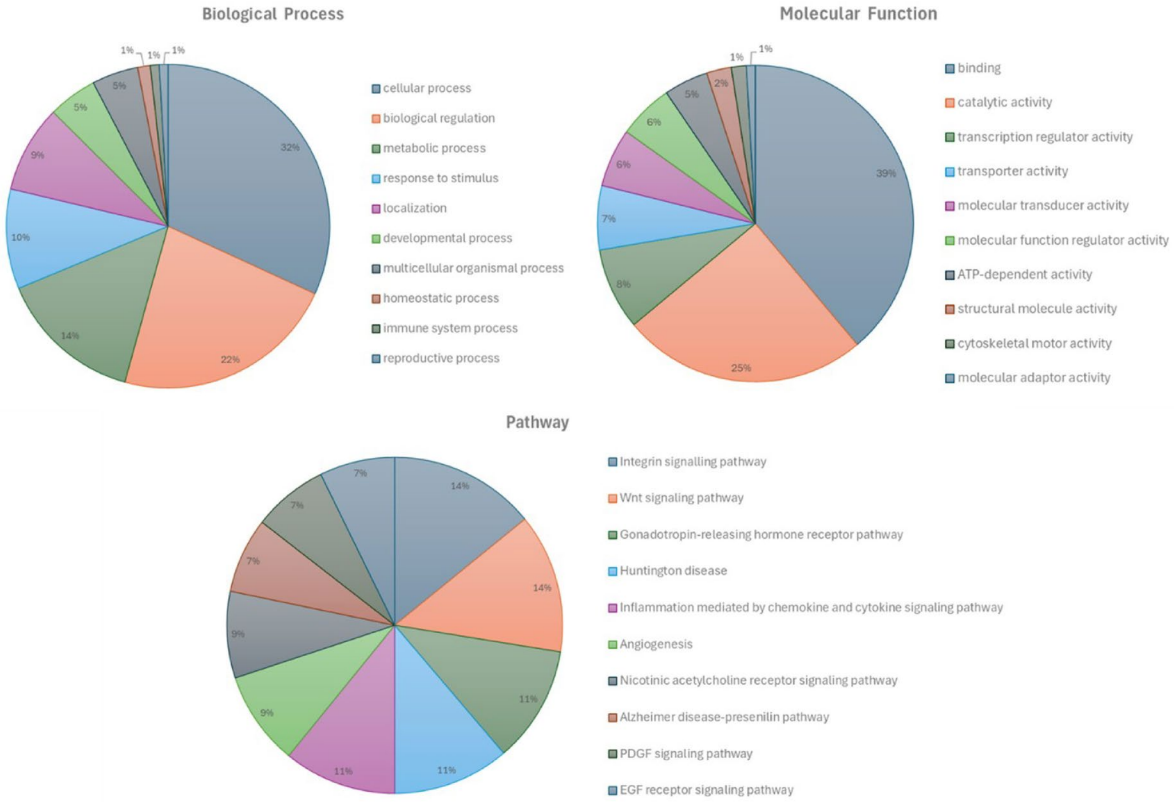


**Fig. 4**. The top 10 biological processes, molecular functions, and pathways identified from the combined proteomic dataset of FIP and non-FIP cats.

corresponds to a sample group. The color gradient indicates the relative protein abundance, where red represents upregulation and blue represents downregulation. The heatmap provides an overall visualization of expression trends and demonstrates a distinct clustering pattern between FIP and non-FIP groups, indicating substantial differences in serum protein profiles between the two conditions. Partial least squares discrimination analysis (PLSDA) was used to compare the data. The PLSDA plot in two dimensions exhibited discernable clusters between the FIP cats (FIP subgroups) and the healthy cats (non-FIP subgroups), as illustrated in Fig. 5b. As shown in Fig. 5c, the score-oriented dendrogram effectively differentiates FIP and non-FIP serum samples based on their unique mass signatures.

To identify the serum proteomic changes in the FIP cats, a binary comparison via volcano plot was conducted to determine the differential analysis. The volcano plot showed the differential protein expression of FIP compared to the healthy cats (Fig. 6). Any change of ≥ fivefold and $p < 0.01$ in protein concentration was considered significant. The volcano plot analysis of the FIP group and the non-FIP group showed that out of 23 proteins, 22 were upregulated (i.e., higher protein concentration in the FIP group) shown in red dots; only one protein was downregulated (i.e., lower protein concentration in the non-FIP group) shown in blue dots (Fig. 6). The gray dots represent no statistically significant differences.

Out of 3384 proteins, 23 candidate proteins were identified, including the calcium-activated potassium channel subunit alpha-1 (M3W870), NIMA-related kinase 3 (A0A5F5XHF7), lactoperoxidase (M3WGL8), RALY heterogenous nuclear ribonucleoprotein (A0A5F5XHL0), FAST kinase domains 2 (M3WMH1), P2X purinoceptor (M3WGZ2), Piwi-like RNA-mediated gene silencing 3 (A0A5F5Y1E9), splicing factor 3B subunit 3 (M3WBJ5), upstream transcription factor family member 3 (M3W304), actin-related protein 2/3 complex subunit 5 (M3WMY0), chromosome B2 C6orf132 homolog (A0A337SGW6), GTPase HRas (M3VZJ0), Ral transcription factor IIIC subunit 1 (M3WCD8), GATOR2 complex protein WDR24 (A0A2I2UZB6), Notch receptor 2 (M3WBU4), polypeptide *N*-acetylgalactosaminyltransferase (M3W5R6), pinin (A0A2I2UZY8), pleckstrin and Sec7 domain containing 2 (A0A2I2V3Y6), exportin-4 (A0A5F5XR08), cadherin 17 (M3WMR7), profilin (M3W1Z0), DNA topoisomerase (A0A2I2UBY3) and SR-related CTD-associated factor 1 (A0A337SL86). Of all 23 differentiated proteins, 22 show upregulation, except for the P2X purinoceptor (M3WGZ2), which shows downregulation in FIP. The assessment of these proteins involved exploring their biological processes, cellular components, and molecular functions using UniProtKB/Swiss-Prot (Table 2).

Further investigation using the online-based STITCH (version 5.0) examined the interaction between differentially expressed proteins and the anti-inflammatory and immunosuppressive drug prednisolone used for treating FIP. Regarding the networks of protein–protein and protein–chemical interactions, as shown in Fig. 7, several candidate proteins represented in this study show a relationship with prednisolone, including lactoperoxidase (LPO), P2X purinoceptor (P2RX7), spicing factor 3b (SF3B3), profilin (PFN1), DNA topoisomerase (TOP3A), Notch receptor 2 (NOTCH2), cadherin 1,7 (CDH17) and RALY heterogenous nuclear ribonucleoprotein (RALY).

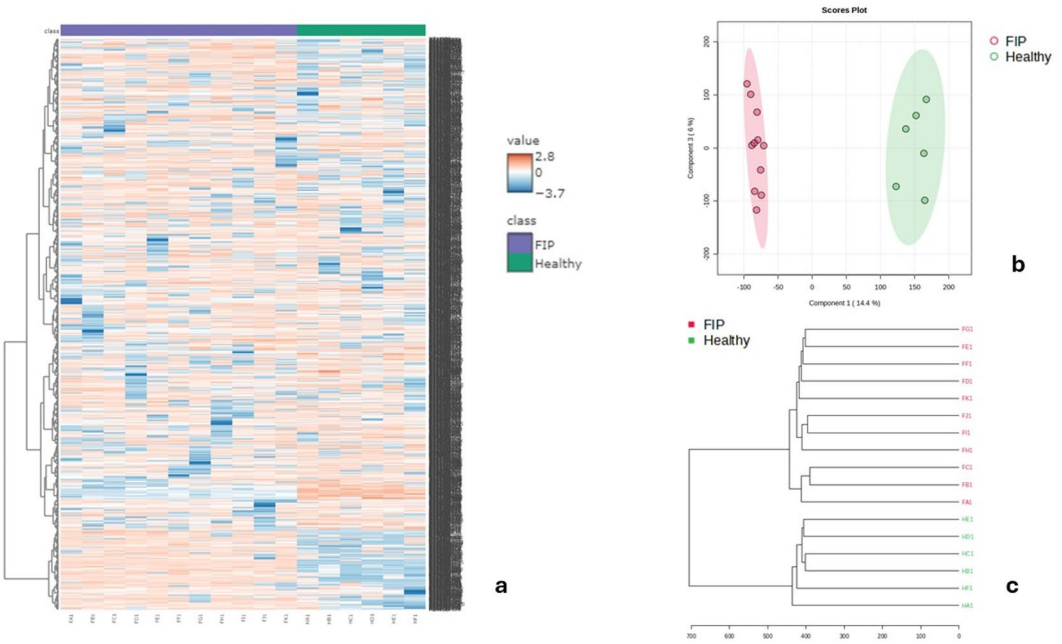


**Fig. 5**. Differential expression analysis of the quantitative proteomics dataset. Heat map of identified serum proteins, with each column indicating a sample and each row indicating a serum protein (**a**). The PLSDA score plot of components one and two, comparing serum samples as they cluster (**b**). The dendrogram demonstrates the protein profile of each group of FIP cats with red letters and non-FIP cats with green letters (**c**).

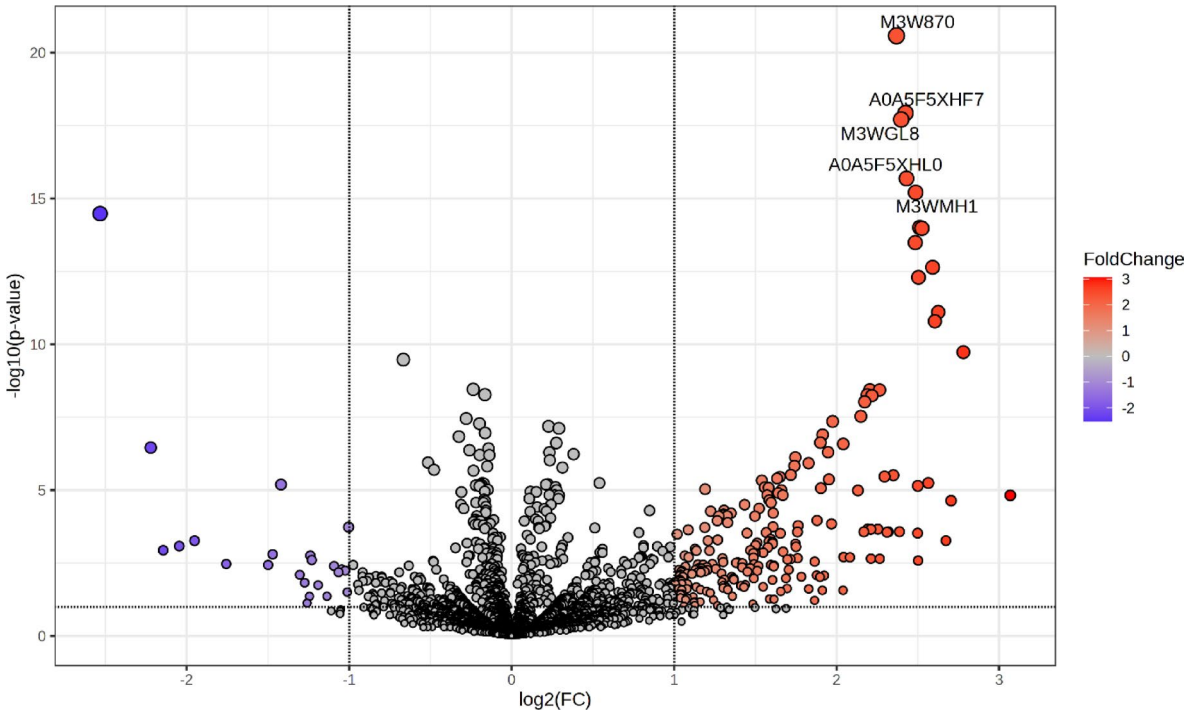


**Fig. 6**. The volcano plot of the binary comparison of differentiated protein expression in FIP vs. non-FIP cats. The significant proteins are shown in red dots (upregulated proteins) or blue (downregulated proteins) with fold change ≥ 5 and $p < 0.01$. The gray dots represent no statistically significant differences in proteins.

## Discussion

FIP is a severe and generally fatal disease in cats caused by virulent mutant forms of FCoV. While most cats, up to 70% worldwide, infected with FCoV remain asymptomatic, a small percentage develop FIP[7,8,27]. The underlying mechanisms of FIP are not fully understood, making the pathogenesis of both the effusive and non-effusive forms of great interest to researchers. To identify potential serum biomarkers, we combined MALDI-TOF for rapid initial screening with LC–MS/MS for more precise protein identification[28]. Candidate proteins were prioritized based on statistical significance, fold change, their association with disease-related signaling pathways, and their correlation with existing literature[29,30]. Twenty-three differentially expressed proteins (22 upregulated, 1 downregulated) demonstrated fold changes greater than or equal to 5 in the FIP group compared to the non-FIP group, with their interactions primarily related to viral infection and immune response pathways.

The pathogenesis of FIP is a systemic inflammatory reaction that could be subacute or chronic, with the effusive form being more acute than the dry form. Chronic inflammation involves the infiltration of macrophages, lymphocytes, and plasma cells, which produce cytokines, growth factors, and enzymes, leading to the formation of granulomas, fibrosis, and tissue damage. FCoV infection results in an increased number of monocytes or macrophages in tissues, which play a central role in FIP pathogenesis, whether FIP develops or not[31]. These cells are essential for the FCoV replication, pyogranuloma formation, and vasculitis seen in FIP. In addition, cats with FIP often experience T-cell depletion in peripheral blood and lymphatic tissues. Hyperglobulinemia occurs, but the humoral immune response contributes to the disease rather than protecting against it. Meanwhile, the downregulation of cell-mediated immunity (CMI) allows uncontrolled viral replication[32]. T-cell depletion and defects in regulation are crucial in FIP development, similar to chronic viral infections in humans where CD8 T cells lose their immune functions[33,34]. Maintaining high-affinity CD8 T cells early in infection is important for virus control and immune restoration[34].

In this study, P2X7, a purinergic receptor, was downregulated in FIP cats compared to healthy controls. P2X purinoceptors, especially P2X4 and P2X7, are generally associated with proinflammatory responses and are frequently upregulated in inflammatory conditions[35]. These ATP-responsive cell surface receptors play critical roles in several physiological and pathological processes, including energy metabolism, immune modulation, and nociception[36]. Altered expression, whether overexpression or decreased expression, of these receptors has been observed in various tumors, infectious diseases, and inflammation-related conditions[36,37]. Interestingly, while P2X receptors are typically linked to proinflammatory effects, adenosine receptor activation induces anti-inflammatory responses[38]. This highlights a complex balance within purinergic signaling, where both pro- and anti-inflammatory components may collaborate to regulate immune responses. Furthermore, many studies have focused on their potential as new therapeutic targets for disease treatment[39,40]. Notably, P2X7 plays a significant role in modulating T-cell function[41]. The downregulation of P2X purinoceptors in FIP cats suggests impaired T-cell activity, which could lead to inadequate immune responses and uncontrolled inflammation. This downregulation may also reflect the altered expression of P2X receptors on immune cells, such as monocytes

| Protein ID | Protein name (gene name) | Peptide sequence | Biological process | Molecular function | FC |
|---|---|---|---|---|---|
| M3W870 | Calcium-activated potassium channel subunit alpha-1 (KCNMA1) | RGGSR | Intracellular potassium ion homeostasis, positive regulation of apoptotic process, vasodilation | Actin binding, voltage-gated potassium channel activity | 5.16 |
| A0A5F5XHF7 | NIMA related kinase 3 (NEK3) | GAKGSALR | Establishment of cell polarity, regulation of tubulin deacetylation | ATP binding, protein kinase activity | 5.37 |
| M3WGL8 | Lactoperoxidase (LPO) | ILGMV | Response to oxidative stress | Heme binding, lactoperoxidase activity | 5.27 |
| A0A5F5XHL0 | RALY heterogenous nuclear ribonucleoprotein (RALY) | SSDGSR | Cholesterol homeostasis, negative regulation of transcription by RNA polymerase II | RNA binding, transcription coregulator activity | 5.39 |
| M3WMH1 | FAST kinase domains 2 (FASTKD2) | GQGVVGGRGR | Apoptotic process, regulation of mitochondrial mRNA stability | RNA binding, rRNA binding | 5.60 |
| M3WGZ2 | P2X purinoceptor (P2RX7) | IVNYSR | Inflammatory response, reactive oxygen species metabolic process, T cell mediated cytotoxicity, T cell proliferation | ATP binding, lipopolysaccharide binding, purinergic nucleotide receptor activity | 0.17 |
| A0A5F5Y1E9 | Piwi like RNA-mediated gene silencing 3 (PNN) | EGNGSNR | Regulation of translation, regulatory ncRNA-mediated gene silencing | RNA binding | 5.75 |
| M3WBJ5 | Splicing factor 3B subunit 3 (SF3B3) | MMTGAGNILK | Negative regulation of protein catabolic process | Protein-containing complex binding, U2 snRNA binding | 5.70 |
| M3W304 | Upstream transcription factor family member 3 (USF3) | ELGTDRR | Negative regulation of epithelial to mesenchymal transition, positive regulation of transcription by RNA polymerase II | DNA-binding transcription activator activity, RNA polymerase II transcription regulatory region sequence-specific DNA binding | 5.59 |
| M3WMY0 | Actin-related protein 2/3 complex subunit 5 (ARPC5) | AVLQSK | Cell migration, regulation of actin filament polymerization | Actin filament binding, structural constituent of cytoskeleton | 6.02 |
| A0A337SGW6 | Chromosome B2 C6orf132 homolog (CB2H6orf132) | GYPGSR | N/A | N/A | 5.67 |
| M3VZJ0 | GTPase Hras (HRAS) | VSPVR | Endocytosis, fibroblast proliferation, T cell receptor signaling pathway, T-helper 1 type immune response | GDP binding, GTP binding, GTPase activity, protein-membrane adaptor activity | 6.17 |
| M3WCD8 | Ral transcription factor IIIC subunit 1 (GTF3C1) | SRGPPR | Transcription initiation at RNA polymerase III promoter | DNA binding, RNA polymerase III general transcription initiation factor activity | 6.08 |
| A0A2I2UZB6 | GATOR2 complex protein WDR24 (WDR24) | ISIHNR | Positive regulation of macroautophagy, Protein K6-linked ubiquitination | Ubiquitin protein ligase activity | 6.87 |
| M3WBU4 | Notch receptor 2 (NOTCH2) | AAKAELEMR | Apoptotic process, inflammatory response to antigenic stimulus, zone B cell differentiation, Notch signaling pathway | N/A | 5.09 |
| M3W5R6 | Polypeptide *N*-acetylgalactosaminyltransferase (GALNT15) | HGESR | Protein O-linked glycosylation | Carbohydrate binding, polypeptide *N*-acetylgalactosaminyltransferase activity | 5.91 |
| A0A2I2UZY8 | Pinin (LOC111558772) | AGGRPQLK | mRNA processing, RNA splicing | DNA binding | 5.66 |
| A0A2I2V3Y6 | Pleckstrin and Sec7 domain containing 2 (PSD2) | GENYR | Regulation of ARF protein signal transduction | Guanyl-nucleotide exchange factor activity, phospholipid binding | 8.39 |
| A0A5F5XR08 | Exportin-4 (XPO4) | SSASGFRR | N/A | Nuclear export signal receptor activity | 6.52 |
| M3WMR7 | Cadherin 17 (CDH17) | LVRMMGVAK | Adherent junction organization, integrin-mediated signaling pathway | Cadherin binding, integrin binding | 5.23 |
| M3W1Z0 | Profilin (PFN4) | AESSGR | Acrosome assembly, manchette assembly, sequestering of actin monomers | Actin monomer binding | 5.65 |
| A0A2I2UBY3 | DNA topoisomerase (TOP3A) | SYSYR | Chromosome separation, DNA topological change, mitochondrial DNA metabolic process | DNA topoisomerase activity, DNA topoisomerase type I (single strand cut, ATP-independent) activity | 6.38 |
| A0A337SL86 | SR-related CTD associated factor 1 (SCAF1) | AGLTSCTR | N/A | RNA polymerase II C-terminal domain binding | 5.66 |

**Table 2**. Candidate protein biomarkers evaluated for biological processes and molecular function by UniProtKB. *FC* fold change between FIP and healthy groups.

and macrophages, during both the early and late stages of FIP. Additionally, studies examining FIPV-infected monocytes, cytokines, and the expression of P2X purinoceptors warrant further investigation. Recent findings report limited but significant increases in granulocyte-monocyte (GM) colony-stimulating factors (CSF) and interleukin-6 (IL-6) in FIPV-infected monocytes, while granulocyte (G)-CSF was upregulated in the mesenteric lymph nodes of FIP-affected cats[42]. This suggests a viral-induced expansion of the monocyte/macrophage population, potentially contributing to immune exhaustion or active host downregulation as part of the viral response. These alterations may result from viral interference, chronic inflammation, or genetic predisposition. P2X7 agonism and blockade are being explored for their potential in treating inflammation and malignancy[43]. Similarly, modulating P2X1 could help restore T-cell function in FIP-affected cats. Overall, further research into P2X receptors in FIP could lead to novel therapeutic approaches. Understanding the mechanisms behind P2X purinoceptor downregulation in FIP cats could provide new strategies for managing and treating the disease, ultimately addressing the molecular deficits that impair immune function.

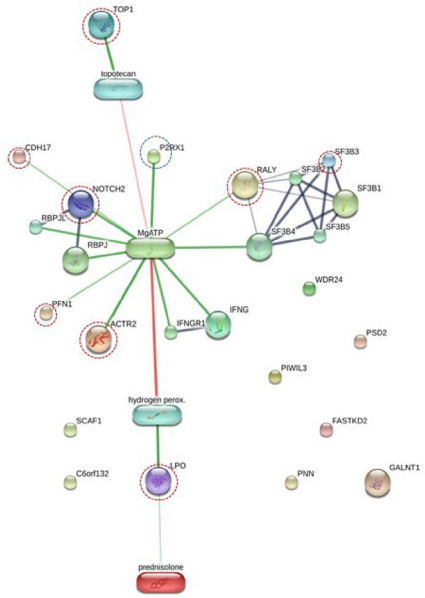


**Fig. 7**. The interaction network of differentially expressed proteins in effusive FIP serum was predicted using the STITCH 5.0 software. Stronger associations are represented by thicker lines. Protein–protein interactions are shown in blue, chemical–protein interactions in green, and interactions between chemicals in red. Eight candidate upregulated proteins associated with the disease are in the red dashed circle, and downregulated proteins are in the blue dashed circle.

Of the 22 upregulated proteins, 8 were linked to prednisolone. Notably, the expression of proteins such as topoisomerases, NOTCH2, and CDH17 is of interest and has been widely reported in biomedical research, suggesting their potential as candidates for the diagnosis and treatment of FIP. DNA topoisomerases are essential enzymes that regulate DNA topology during replication and transcription by relieving torsional stress. Recently, topoisomerases have gained attention for their tissue-specific roles, particularly in immune homeostasis[44]. The mammalian genome contains seven genes that encode topoisomerases: four for type I topoisomerases (TOP1, TOP1mt, TOP3A, and TOP3B) and three for type II topoisomerases (TOP2A, TOP2B, and SPO11)[44]. Previous research has demonstrated that during many bacterial and viral infections and coinfections, the host enzyme topoisomerase 1 (TOP1) is necessary to fully transactivate infection-induced genes and hence regulate the formation of inflammatory gene programs[45]. Moreover, therapeutic administration of topoisomerase inhibitors after infection has been shown to rescue mortality in animal models of inflammation-induced death[45]. As found previously, TOP1 has been reported as an accessible therapy against lethal inflammation from SARS-CoV-2 in animal models[46]. The progression of FIP shares similarities with severe COVID-19, as both diseases exhibit an initial phase of rising viremia followed by a decline, and a subsequent phase marked by a rapid increase in systemic inflammation[42,47]. Partially suppressing antiviral and inflammatory genes in infected cells can block virus replication while preventing excessive inflammation. In contrast, immune cells that respond to pathogen-associated or damage-associated signals may trigger excessive inflammation. Understanding these mechanisms provides valuable insights for developing targeted therapies.

The NOTCH2 gene is part of a family of genes that encode transmembrane receptors in the highly conserved Notch signaling pathway, which is crucial for many developmental processes[48]. This signaling system allows cells to communicate and regulate key processes, such as apoptosis, cell differentiation, and proliferation under different physiological conditions[49,50]. It has been shown that TNF-alpha, a proinflammatory cytokine, specifically regulates the Notch pathway in vascular endothelial cells (ECs)[51]. This regulation aligns with the role of TNF-alpha in FIP, where it upregulates the expression of the FIPV receptor feline aminopeptidase N in feline macrophages, contributing to the disease's progression[52]. The Notch pathway, including NOTCH2, is involved in various stages of blood vessel development and inflammatory-related vascular injury and remodeling processes, such as vasculitis[53]. FIP is characterized by immune-mediated vasculitis driven by macrophage/monocyte activation, and the upregulation of NOTCH2 could be linked to this mechanism. NOTCH molecules exhibit a pattern of expression changes in disease, with decreased NOTCH4 and increased NOTCH2 expression[54]. NOTCH2 is also expressed in a variety of human tumor cells and in feline lymphoma associated with FeLV infection[48,54–56]. Therefore, the upregulation of NOTCH2 in cats with FIP suggests that this receptor could play a role in the pathogenesis of the disease by influencing immune responses and inflammation and contributing to immune-mediated vasculitis.

The cadherin family of adhesion molecules regulates cell–cell interactions. CDH17, a member of the 7D-cadherin superfamily, is a transmembrane protein primarily involved in cell adhesion, particularly in the gastrointestinal tract[57]. It has been implicated in various cancers, especially in the GI tract, and is associated with processes such as cell proliferation, migration, and invasion, making it a potential treatment target in

humans[58–60]. The upregulation of CDH17 in cats with FIP compared to healthy cats suggests several potential roles in the pathogenesis of FIP. This upregulation may influence cell adhesion, migration, and immune response, potentially contributing to granuloma formation and chronic inflammation in FIP. Additionally, it may be linked to the tissue remodeling or fibrosis observed in FIP, particularly in the liver and intestines, where CDH17 is normally expressed. To date, there is limited published research directly linking CDH17 to feline diseases, suggesting that these findings could represent a novel aspect of disease pathology. Further research is needed to evaluate this potential association. Therefore, exploring the role of CDH17 in FIP could provide new insights into how cell adhesion and migration contribute to the disease's progression.

Although RT-PCR was used in most cases to detect FCoV in effusion samples, several cats tested negative. However, these cases were diagnosed based on a combination of consistent clinical signs, positive Rivalta's test, cytological findings, and FCoV antibody detection. This approach is supported by prior studies indicating that RT-PCR may yield false-negative results even in cats with confirmed FIP[7,9]. Necropsy was performed in three cats, which confirmed the diagnosis.

In addition to CDH17, the proteomic analysis also identified serum amyloid A (SAA), an acute phase protein that is known to increase in cats with FIP. This finding aligns with previous studies highlighting the inflammatory nature of FIP[10,11]. However, other commonly reported acute phase proteins such as alpha-1-acid glycoprotein (AGP) and haptoglobin were not detected. This may be attributed to low expression levels, the limitations of mass spectrometry sensitivity, or incomplete annotation of feline proteins in the reference database. Nonetheless, these proteins remain biologically relevant in the context of FIP and warrant further investigation.

Additionally, 15 other proteins that were not significantly related to this signaling pathway were identified. Examples include SR-related CTD-associated factor 1 (SCAF1), GATOR2 complex protein WDR24 (WDR24), and FAST kinase domain-containing protein 2 (FASTKD2). Further studies are necessary to validate whether these and other identified proteins could serve as novel biomarkers for cats with FIP in the future.

This study reports proteomic findings on FIP from the perspective of protein expression. However, it has some limitations. First, necropsies could not be performed on all FIP cases due to owner refusal and loss of follow-up. Second, it was challenging to fully control for various factors, such as age, sex, breed, and previous treatment with anti-inflammatory drugs, which might have been prescribed in some cases before the cats visited KUVTH. Finally, our study pooled serum samples followed by peptide mass fingerprinting, which meant that samples from pleural and peritoneal effusions could be included in the same subgroup but were all evaluated as FIP serum. For more understanding, future research should differentiate between pleural and peritoneal effusions and study all proteomes in the serum, effusion, and tissue of FIP. Moreover, the candidate proteins identified in this study were not further validated by immunodetection methods such as Western blot or ELISA due to technical limitations, including the lack of feline-specific antibodies and limited residual serum volume. Future studies using independent confirmation methods will be important to verify the diagnostic value of these potential biomarkers.

## Conclusion

This study represents the first investigation of serum proteome profiling in cats with FIP, providing insight into potential FIP biomarkers. The discovery and assessment of new protein candidates, particularly P2X purinoceptors, DNA topoisomerases, NOTCH2, and CDH17 in cats with FIP, offer a valuable foundation for future research. These findings pave the way for the development of novel diagnostic methods and targeted therapies. However, these results are preliminary and require further validation.

## Data availability

The MS/MS raw data and analysis files have been deposited in the ProteomeXchange Consortium (http://proteomecentral.proteomexchange.org) via the jPOST partner repository (https://jpostdb.org) with the dataset identifiers JPST003448 and PXD057397. For reviewers, a preview is available at https://repository.jpostdb.org/preview/6541863896724260dd42f3 (Access key: 7548). All relevant data are included within the manuscript and its supporting information files.

Received: 13 November 2024; Accepted: 19 May 2025
Published online: 29 May 2025

## References

1. Holzworth, J. Some important disorders of cats. *Cornell Vet.* **53**, 157–160 (1963).
2. Pedersen, N. C. A review of feline infectious peritonitis virus infection: 1963–2008. *J. Feline Med. Surg.* **11**, 225–258 (2009).
3. Paltrinieri, S., Cammarata, M. P., Cammarata, G. & Comazzi, S. Some aspects of humoral and cellular immunity in naturally occurring feline infectious peritonitis. *Vet. Immunol. Immunopathol.* **65**, 205–220 (1998).
4. Pedersen, N. C. et al. Efficacy and safety of the nucleoside analog GS-441524 for treatment of cats with naturally occurring feline infectious peritonitis. *J. Feline Med. Surg.* **21**, 271–281 (2019).
5. Roy, M. et al. Unlicensed molnupiravir is an effective rescue treatment following failure of unlicensed GS-441524-like therapy for cats with suspected feline infectious peritonitis. *Pathogens* **11**, 1209 (2022).
6. Thayer, V. et al. 2022 AAFP/EveryCat feline infectious peritonitis diagnosis guidelines. *J. Feline Med. Surg.* **24**, 905–933 (2022).
7. Tasker, S. et al. Feline infectious peritonitis: European advisory board on cat diseases guidelines. *Viruses* **15**, 1847 (2023).
8. Moyadee, W. et al. Feline infectious peritonitis: A comprehensive evaluation of clinical manifestations, laboratory diagnosis, and therapeutic approaches. *J. Adv. Vet. Anim. Res.* **11**, 19 (2024).
9. Felten, S. et al. Sensitivity and specificity of a real-time reverse transcriptase polymerase chain reaction detecting feline coronavirus mutations in effusion and serum/plasma of cats to diagnose feline infectious peritonitis. *BMC Vet. Res.* **13**, 1–11 (2017).
10. Romanelli, P. et al. Measurement of feline alpha-1 acid glycoprotein in serum and effusion using an ELISA method: Analytical validation and diagnostic role for feline infectious peritonitis. *Pathogens* **13**, 289 (2024).

11. Hazuchova, K., Held, S. & Neiger, R. Usefulness of acute phase proteins in differentiating between feline infectious peritonitis and other diseases in cats with body cavity effusions. *J. Feline Med. Surg.* **19**, 809–816 (2017).
12. Meazzi, S. et al. Role of paraoxonase-1 as a diagnostic marker for feline infectious peritonitis. *Vet. J.* **272**, 105661 (2021).
13. Rossi, G. Acute phase proteins in cats: Diagnostic and prognostic role, future directions, and analytical challenges. *Vet. Clin. Pathol.* **52**, 37–49 (2023).
14. Tothova, C., Nagy, O. & Kovac, G. Serum proteins and their diagnostic utility in veterinary medicine: A review. *Vet. Med.* **61**, 475–496 (2016).
15. Mayne, E. S., George, J. A. & Louw, S. Assessing biomarkers in viral infection. *Adv. Exp. Med. Biol.* **1412**, 159–173 (2023).
16. Sperk, M. et al. Utility of proteomics in emerging and re-emerging infectious diseases caused by RNA viruses. *J. Proteome Res.* **19**, 4259–4274 (2020).
17. Urbiola-Salvador, V., Lima de Souza, S., Macur, K., Czaplewska, P. & Chen, Z. Plasma proteomics elucidated a protein signature in COVID-19 patients with comorbidities and early-diagnosis biomarkers. *Biomedicines* **12**, 840 (2024).
18. Ferlizza, E. et al. The effect of chronic kidney disease on the urine proteome in the domestic cat (*Felis catus*). *Vet. J.* **204**, 73–81 (2015).
19. Meachem, M. D. et al. Comparative proteomic study of plasma in feline pancreatitis and pancreatic carcinoma using 2-dimensional gel electrophoresis to identify diagnostic biomarkers: A pilot study. *Can. J. Vet. Res.* **79**, 184–189 (2015).
20. Liu, M. et al. Novel biomarkers in cats with congestive heart failure due to primary cardiomyopathy. *J. Proteom.* **226**, 103896 (2020).
21. Yu, J. et al. Serum proteome profiles in cats with chronic enteropathies. *J. Vet. Intern. Med.* **37**, 1358–1367 (2023).
22. Lowry, O. H., Rosebrough, N. J., Farr, A. L. & Randall, R. J. Protein measurement with the Folin phenol reagent. *J. Biol. Chem.* **193**, 265–275 (1951).
23. Johansson, C. et al. Differential expression analysis of *Escherichia coli* proteins using a novel software for relative quantitation of LC–MS/MS data. *Proteomics* **6**, 4475–4485 (2006).
24. Thorsell, A., Portelius, E., Blennow, K. & Westman, B. A. Evaluation of sample fractionation using microscale liquid-phase isoelectric focusing on mass spectrometric identification and quantitation of proteins in a SILAC experiment. *Rapid Commun. Mass Spectrom.* **21**, 771–778 (2007).
25. Perkins, D. N., Pappin, D. J., Creasy, D. M. & Cottrell, J. S. Probability-based protein identification by searching sequence databases using mass spectrometry data. *Electrophoresis* **20**, 3551–3567 (1999).
26. Szklarczyk, D. et al. STITCH 5: augmenting protein–chemical interaction networks with tissue and affinity data. *Nucleic Acids Res.* **44**, 380–384 (2016).
27. Dong, B. et al. Prevalence of natural feline coronavirus infection in domestic cats in Fujian, China. *Virol. J.* **21**, 2 (2024).
28. Ploypetch, S. et al. Utilizing MALDI-TOF MS and LC–MS/MS to access serum peptidome-based biomarkers in canine oral tumors. *Sci. Rep.* **12**, 21641 (2022).
29. Gajula, S. N. et al. LC-MS/MS: A sensitive and selective analytical technique to detect COVID-19 protein biomarkers in the early disease stage. *Expert Rev. Proteom.* **20**, 5–18 (2023).
30. Nakayasu, et al. Tutorial: Best practices and considerations for mass-spectrometry-based protein biomarker discovery and validation. *Nat. Protoc.* **8**, 3737–3760 (2021).
31. Gao, Y. Y. An updated review of feline coronavirus: Mind the two biotypes. *Virus Res.* **326**, 199059 (2023).
32. Malbon, A. J. et al. The effect of natural feline coronavirus infection on the host immune response: A whole-transcriptome analysis of the mesenteric lymph nodes in cats with and without feline infectious peritonitis. *Pathogens* **9**, 524 (2020).
33. Paltrinieri, S., Ponti, W., Comazzi, S., Giordano, A. & Poli, G. Shifts in circulating lymphocyte subsets in cats with feline infectious peritonitis (FIP): Pathogenic role and diagnostic relevance. *Vet. Immunol. Immunopathol.* **9**, 141–148 (2003).
34. Brooks, D. G., Tishon, A., Oldstone, M. B. & McGavern, D. B. Prevention of CD8 T cell deletion during chronic viral infection. *Viruses* **13**, 1189 (2021).
35. Liu, J. P. et al. ATP ion channel P2X purinergic receptors in inflammation response. *Biomed. Pharmacother.* **158**, 114205 (2023).
36. Hughes, J. P., Hatcher, J. P. & Chessell, I. P. The role of P2X 7 in pain and inflammation. *Purinergic Signal* **3**, 163–169 (2007).
37. Li, X. et al. Decreased expression of P2X7 in endometrial epithelial pre-cancerous and cancer cells. *Gynecol. Oncol.* **106**, 233–243 (2007).
38. Soare, A. Y. et al. P2RX7 at the host–pathogen interface of infectious diseases. *Microbiol. Mol. Biol.* **85**, 10–1128 (2021).
39. Burnstock, G. & Knight, G. E. The potential of P2X7 receptors as a therapeutic target, including inflammation and tumour progression. *Purinergic Signal* **14**, 1–8 (2018).
40. Sophocleous, R. A. et al. Pharmacological and genetic characterisation of the canine P2X4 receptor. *Br. J. Pharmacol.* **177**, 2812–2829 (2020).
41. Grassi, F. The P2X7 receptor as regulator of T cell development and function. *Front. Immunol.* **11**, 1179 (2020).
42. Malbon, A. J. et al. Colony stimulating factors in early feline infectious peritonitis virus infection of monocytes and in end stage feline infectious peritonitis; A combined in vivo and in vitro approach. *Pathogens* **9**, 893 (2020).
43. Zabłocki, K. & Górecki, D. C. The role of P2X7 purinoceptors in the pathogenesis and treatment of muscular dystrophies. *Int. J. Mol. Sci.* **24**, 9434 (2023).
44. Muralidhara, P., Kumar, A., Chaurasia, M. K. & Bansal, K. Topoisomerases in immune cell development and function. *J. Immunol.* **210**, 126–133 (2023).
45. Rialdi, A. et al. Topoisomerase 1 inhibition suppresses inflammatory genes and protects from death by inflammation. *Science* **352**, aad7993 (2016).
46. Ho, J. S. et al. TOP1 inhibition therapy protects against SARS-CoV-2-induced lethal inflammation. *Cell* **184**, 2618–2632 (2021).
47. Merad, M. & Martin, J. C. Pathological inflammation in patients with COVID-19: A key role for monocytes and macrophages. *Nat. Rev. Immunol.* **20**, 355–362 (2020).
48. Pancewicz, J. A brief overview of clinical significance of novel Notch2 regulators. *Mol. Cell. Oncol.* **7**, 1776084 (2020).
49. Hansson, E. M., Lendahl, U. & Chapman, G. Notch signaling in development and disease. *Semin. Cancer Biol.* **14**, 320–328 (2004).
50. Di Stefano, A. et al. Upregulation of notch signaling and cell-differentiation inhibitory transcription factors in stable chronic obstructive pulmonary disease patients. *Int. J. Mol. Sci.* **25**, 3287 (2024).
51. Quillard, T., Devallière, J., Couple, S. & Charreau, B. Inflammation dysregulates Notch signaling in endothelial cells: Implication of Notch2 and Notch4 to endothelial dysfunction. *Biochem. Pharmacol.* **80**, 2032–2041 (2010).
52. Takano, T., Hohdatsu, T., Toda, A., Tanabe, M. & Koyama, H. TNF-alpha, produced by feline infectious peritonitis virus (FIPV)-infected macrophages, upregulates expression of type II FIPV receptor feline aminopeptidase N in feline macrophages. *Virology* **364**, 64–72 (2007).
53. Quillard, T. & Charreau, B. Impact of notch signaling on inflammatory responses in cardiovascular disorders. *Int. J. Mol. Sci.* **14**, 6863–6888 (2013).
54. Mesini, N. et al. Role of Notch2 pathway in mature B cell malignancies. *Front. Oncol.* **12**, 1073672 (2023).
55. Rohn, J. L., Lauring, A. S., Linenberger, M. L. & Overbaugh, J. Transduction of Notch2 in feline leukemia virus-induced thymic lymphoma. *J. Virol.* **70**, 8071–8080 (1996).
56. Watanabe, S. et al. Notch2 transduction by Feline leukemia virus in a naturally infected cat. *J. Vet. Med. Sci.* **76**, 553–557 (2014).
57. Lee, N. P., Poon, R. T., Shek, F. H., Ng, I. O. & Luk, J. M. Role of cadherin-17 in oncogenesis and potential therapeutic implications in hepatocellular carcinoma. *Biochim. Biophys. Acta* **1806**, 138–145 (2010).

58. Wang, J. et al. Cadherin-17 induces tumorigenesis and lymphatic metastasis in gastric cancer through activation of NFκB signaling pathway. *Cancer Biol.* **14**, 262–270 (2013).
59. Long, Z. W., Zhou, M. L., Fu, J. W., Chu, X. Q. & Wang, Y. N. Association between cadherin-17 expression and pathological characteristics of gastric cancer: a meta-analysis. *World J. Gastroenterol.* **21**, 3694 (2015).
60. Delaney, S. et al. Cadherin-17 as a target for the immunoPET of adenocarcinoma. *Eur. J. Nucl. Med. Mol. Imaging* **16**, 1–11 (2024).

## Acknowledgements
The authors thank all staff of the feline clinic, blood bank unit, emergency room, and outpatient department (OPD) at the Kasetsart University Veterinary Teaching Hospital, Faculty of Veterinary Medicine, Kasetsart University, Bangkhen Campus, for their invaluable assistance with sample collection.

## Author contributions
J.R. designed the overall study concept and supervised the project. J.R. and N.T. were responsible for funding acquisition. W.M. collected samples, performed experiments, and wrote the manuscript. S.R., J.J., N.P., and W.M. carried out proteomic analysis using MALDI-TOF and LC–MS/MS. J.R., S.R., S.P., N.T., and WM analyzed the data. J.R., S.R., K.C., N.T., and A.R. reviewed and revised the manuscript. All authors read and approved the final manuscript.

## Funding
This research project is supported by the National Research Council of Thailand (NRCT): NRCT5-RGJ63002-039 and Faculty of Veterinary Medicine, Kasetsart University.

## Declarations

## Competing interests
The authors declare no competing interests.

## Ethics approval and consent participate
The work described in this manuscript involved the use of non-experimental (owned) animals. The study received prior ethical approval from the Kasetsart University Institutional Animal Care and Use Committee, Kasetsart University, Bangkok, Thailand, which approved all procedures involving animal use (approval number: ACKU66-VET-019). This study is reported in accordance with ARRIVE guidelines. All methods were conducted in accordance with relevant guidelines and regulations for reporting animal experiments. Blood for proteomic analysis was collected during routine veterinary examinations. Serum samples were obtained from the patients with signed informed consent forms from their owners, and a high standard of care was maintained throughout each examination.

## Additional information
**Supplementary Information** The online version contains supplementary material available at https://doi.org/10.1038/s41598-025-03108-2.

**Correspondence** and requests for materials should be addressed to J.R.

**Reprints and permissions information** is available at www.nature.com/reprints.

**Publisher's note** Springer Nature remains neutral with regard to jurisdictional claims in published maps and institutional affiliations.